Food Chemistry: X 26 (2025) 102341

Contents lists available at ScienceDirect

Food Chemistry: X

journal homepage: www.sciencedirect.com/journal/food-chemistry-x

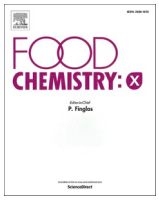

High molecular weight soluble dietary fiber of corn bran exhibits stronger inhibitions in digestibility and short-term retrogradation of corn starch than low molecular weight soluble fiber

Yuqian Zheng [a,1], Lixin You [b,1], Wenyan Wang [a], Xiaoyan Qin [a], Zhilong Chen [a], Ruining Zhang [c], Jun Zhao [a], Sheng Li [a,*]

[a] College of Food Sciences and Engineering, Changchun University, Changchun, 130022, China
[b] School of Life Science, Changchun Sci-Tech University, Changchun, Jilin 130600, China
[c] Agriculture College, Yanbian University, Yanbian 133002, China

ARTICLE INFO

Keywords:
Starch
Molecular weight
Pasting properties
Retrogradation properties

ABSTRACT

Starch-dietary fiber interactions regulate starch processing and digestion, though the effects of varying molecular weight dietary fibers remain insufficiently studied. This study investigates how corn bran-derived soluble dietary fibers (SDFs) with distinct molecular weights influence corn starch (CS) processing, retrogradation, and digestibility. Results revealed that adding 5 % (*W*/W, based on the dry weight of CS) high molecular weight soluble dietary fiber (HM-SDF) or low molecular weight soluble dietary fiber (LM-SDF) significantly reduced amylose leaching, peak viscosity, retrogradation value, and retrogradation enthalpy during CS pasting. HM-SDF and LM-SDF decreased the thixotropic ring area by 55.8 % and 16.5 %, respectively, and inhibited the formation of ordered structures in CS. The HM-SDF-CS complex contained the least rapidly digestible starch at 68.26 %, indicating it more effectively slows starch digestion. These findings enhance our understanding of how SDF molecular weight distribution modulates starch-based foods, offering insights into potential applications for improved food processing and digestibility.

1. Introduction

Starch is a natural polysaccharide composed of glucose units linked by α-1,4 and α-1,6 glycosidic bonds. It is commonly found in the tubers and seeds of various plants. Corn starch (CS) is widely used in the food industry as a gelling agent, thickener, and fat replacer due to its low cost. However, natural corn starch (NCS) has several limitations, including poor shear resistance, susceptibility to aging, and a high glycemic index, which restricts its broader application. Starch can be classified based on its digestibility into rapidly digestible starch (RDS), slowly digestible starch (SDS), and resistant starch (RS). SDS and RS are beneficial in lowering blood glucose and providing fewer or no calories, which can reduce the risk of chronic diseases (Lee et al., 2019). Its rapid digestion can lead to increased blood glucose levels. Modifying starch digestion can help mitigate this response, reducing blood glucose spikes. Diverse modification techniques for starches are key to enhancing their nutritional and functional profiles.

Effective methods for modifying starch include physical, chemical, and biological (enzyme-based) approaches (Lee et al., 2019). Among these, physical modification has gained significant attention due to its environmental benefits, cost-effectiveness, and safety. Physical modification of starch with non-starch components (polysaccharides, fatty acids, salts and plant extracts) can change the structure and properties of starch (Jia et al., 2022). Of these ingredients, polysaccharides are particularly valued for their biocompatibility and are commonly used to reduce starch retrogradation in food products. Previous studies have shown that polysaccharides like Laminaria japonica(Zhou et al., 2022), chitosan(Liu et al., 2019), guar gum(Zheng et al., 2019), and konjac glucomannan(S. Ma, P. Zhu, & M. Wang 2019) influence the processing, retrogradation, and digestive properties of starch-based foods. Laminaria japonica polysaccharides inhibited wheat starch retrogradation and reduced the storage modulus, loss modulus, and pasting index of wheat starch(Zhou et al., 2022). Adding chitosan reduced the viscosity of maize-resistant starch, whereas adding linseed gum, xanthan gum,

* Corresponding author.
E-mail address: lish92@ccu.edu.cn (S. Li).
[1] Yuqian Zheng and Lixin You indicates that they are co-first authors

https://doi.org/10.1016/j.fochx.2025.102341
Received 31 December 2024; Received in revised form 24 February 2025; Accepted 27 February 2025
Available online 8 March 2025

and konjac gum increased the viscosity(Liu et al., 2019). The addition of guar gum to autoclaved and cooled lotus starch resulted in the formation of a denser crystal structure and reduced digestibility(Zheng et al., 2019). Konjac glycans significantly altered the pasting and rheological properties of maize starch, increased the pasting temperature and peak viscosity, and increased the storage modulus and loss modulus of maize starch(S. Ma, P. Zhu, & M. Wang 2019).

In addition to the type of polysaccharide, its molecular weight plays a crucial role in modifying starch behavior. For example, low-molecular-weight pectin is more effective at inhibiting retrogradation, while high-molecular-weight konjac glucomannan is more successful in preventing starch retrogradation and reducing starch gel dehydration and contraction(S. Luo et al., 2017; S. Ma, P. Zhu, M. Wang, et al., 2019). Different molecular weight non-starch polysaccharides also had different effects on the rheological properties of starch. The larger molecular weight of jicama non-starch polysaccharides promoted the leaching of amylose from jicama starch and formed a denser and more homogeneous gel network structure(Huang et al., 2023).

Dietary fibers are frequently used in starch modification because they minimally affect the crystalline structure of starch. They improve crystallinity, water-holding capacity, and rheological properties while also being adaptable to specific food processing needs. Their effect on starch gel properties is also easier to control. Soluble dietary fibers (SDFs), such as pectin, guar gum, sodium alginate, and polydextrose, are commonly added to starch-based foods to act as thickeners and emulsifiers. They enhance food quality and storage by regulating moisture mobility. Starch retrogradation is a key factor influencing the quality and shelf-life of starch-based foods. However, the mechanisms by which dietary fibers inhibit starch retrogradation are complex and influenced by various factors. The impact of SDFs on corn starch (CS) properties depends on several variables, including the type, source, preparation method, molecular weight, and the conditions of pasting and retrogradation. While much research has focused on the effects of different dietary fiber sources on starch processing, retrogradation, and digestion, there is limited information on how dietary fibers with varying molecular weights affect starch pasting, retrogradation, and in vitro digestion.

There is a growing market demand for starch-SDF complexes with enhanced retrogradation resistance with a further increase in awareness about dietary fibers and in demand for food products with low glycemic index (Li, Liu, et al., 2022; Liu et al., 2019). The addition of starch-SDF complexes enhances the anti-resorption properties of bakery products, extends shelf life, and improves product quality (Fatimah et al., 2024). When applied to beverages, it improves the stability and taste of beverages, increases the dietary fiber content of beverages, and meets consumer demand for healthy beverages (Li, Liu, et al., 2022). Adding the complex to instant noodles can reduce the sticking phenomenon during the brewing process and improve the texture of the noodles (Bhatta, 2023). However, a deeper understanding of how different molecular weights of dietary fibers affect various properties of starch is still needed. In this study, two SDFs with varying molecular weights were prepared through an ethanol precipitation method using different ethanol concentrations. The effects of these fibers on the gel properties of CS, including pasting, static rheological, and dynamic rheological properties, were systematically examined. Additionally, the study explored how dietary fibers of different molecular weights influence starch processing, retrogradation, and digestibility. The findings aim to provide insights into how molecular weight affects starch retrogradation, offering valuable knowledge for developing starch-based foods with reduced retrogradation and improved digestibility through physical modification.

2. Materials and methods

2.1. Materials

Twin-screw extruded-enzymatically prepared soluble dietary fibers (EESDF) were prepared from corn bran by the methods of Li, Hu, et al. (2022). Corn bran was bought from Changchun Dacheng Biotechnology Development Co (Changchun, China). Corn starch (CS) (product code: RT1152, 27.54 % amylose content, 15.41 % moisture content) was purchased from Shanghai RYON Biotechnology Co (Shanghai, China). Heat-resistant α-amylase (A109182, 3400 U/mL) was purchased from Aladdin Reagent (Shanghai, China). Alkaline protease (A10154, from *Bacillus licheniformis*, 200 U/mg) was bought from Genye Biotechnology Co (Guangzhou, China). Amyloglucosidase (A800618, from *Aspergillus niger*, 100,000 U/mL) was bought from McLean Biochemical Technology Co. (Shanghai, China). All other chemicals and reagents used in this study were of analytical grade.

2.2. Preparation of SDFs with different molecular weights

SDFs prepared by twin-screw-enzymatic modification(Li, Hu, et al., 2022) were used as raw materials. We dissolved the raw materials in deionized water to prepare a 10 % concentration solution. Then we slowly added the anhydrous ethanol to the solution, increasing the ethanol concentration to 40 % and 80 % (Xue et al., 2019a). The precipitates were obtained freeze-dried and named HM-SDF and LM-SDF.

2.3. Monosaccharide composition of different fractions of SDFs

The composition of monosaccharides was determined by high performance liquid chromatography (HPLC). The measurement conditions are as follows: Diamonsil C18 column (250 mm × 4.6 mm, 5 μm), mobile phase A: phosphate buffer (pH 6.8): acetonitrile (85,15, *v*/v), mobile phase B: PBS (pH 6.8): acetonitrile (60,40, v/v), flow rate: 0.9 mL/min, column temperature: 40 °C, detection wavelength: 250 nm, injection Volume: 10 μL. A 20 mg sample was hydrolyzed with 2 mol/L trifluoroacetic acid at 110 °C for 8 h. 6 mL of 0.5 mol/L methanol PMP (1-phenyl-3-methyl-5-pyrazolone) solution and 5 mL of 0.3 mol/L sodium hydroxide solution were added to the hydrolyzed solution, and the extract was extracted in a water bath at 70 °C for 1 h. The extracted samples were cooled, neutralized with 5 mL of 0.3 mol/L hydrochloric acid, and extracted three times with an equal volume of chloroform. The 0.45 μm membrane-filtered aqueous layer was used for HPLC analysis.

2.4. Molecular weight determination of different fractions of SDFs

Molecular weights were determined by using high-performance gel permeation chromatography (HPGPC) according to the method of Gan et al. (2020) with minor modifications. The mobile phase of the sample solution (10 mg/mL) was configured using 0.7 % Na_2SO_4. The standard curve was produced by Dextran T standard (*Mw*: 10 kDa, 40 kDa, 70 kDa, 500 kDa, 2000 kDa) and glucose. The solution was filtered through a 0.45 μm membrane and analyzed at 35 °C (column temperature autocontrol system) on an SRT SEC-100 column (7.8 × 300 mm, 5 μm, Sepax, USA) with RID-20 A at a flow rate of 2.5 mL/min. The molecular weight of SDF samples was determined using a standard curve derived from a known molecular weight T-series Dextran standard.

2.5. Preparation of samples

3 g of CS powder was mixed with 5 % HM-SDF and 5 % LM-SDF powders (*W*/W, based on the dry weight of CS), respectively (Y.-S. Ma et al., 2019). All mixtures have a dry storage life at room temperature to perform the following determinations.

2.6. Determination of pasting properties

The pasting properties of the starch systems were evaluated using a rapid viscosity analyzer (RVA) (RVATECMASTER, Perten Instruments Ltd., Sweden). Take 3 g of the samples (CS, CS-HM-SDF, and CS-LM-SDF) add 25 mL of distilled water, and stir evenly in an RVA aluminum

cylinder. The samples were measured using the RVA Standard 1 method. After stirring at 50 °C and 960 rpm (10 s), the samples were subjected to a heating and cooling cycle for 12 min. The peak viscosity, through viscosity, breakdown viscosity, final viscosity, setback viscosity, and peak time were then recorded by instrumental measurements. The pasting curves of the samples were obtained using RVA (Zhao et al., 2021).

2.7. Determination of leaching amylose content

The leaching content of amylose was measured using the iodine colorimetric method (Funami et al., 2005). Before the test, the samples (CS, CS-HM-SDF, and CS-LM-SDF) were bathed in water at 90 °C and centrifuged at 10000 ×*g* for 20 min. To prepare the solution, add 0.5 % trifluoroacetic acid and carefully adjust the pH to 5.5. Subsequently, incorporate 50 μL of I_2-KI solution at a concentration of 0.01 mol/L for staining purposes. Finally, adjust the total volume of the mixture to 50 mL. Absorbance values were measured at 620 nm after 30 min at room temperature (deionized water for the blank control group).

2.8. Determination of rheological properties

The samples after the RVA test were left at 25 °C for 5 min. The static rheological and dynamic rheological properties were determined using a rheometer (MCR302, Anton Paar, Austria) with a stainless steel parallel plate (25 mm in diameter). The static shear flow behavior was measured as follows: the gap was set to 1.0 nm, and the measurement temperature was 25 °C. Samples with a stable flow behavior were measured at shear rates from 0.1 s^{-1} to 300 s^{-1}. The shear stress and viscosity were recorded as a function of shear rate(Wu et al., 2013). The experimental data were fitted using the power law model:

$$\tau = k\gamma^n \quad (1)$$

In the model, τ (Pa) is the shear stress, k (Pa·s^n) is the consistency coefficient, γ (s^{-1}) is the shear rate, and n is the flow behavior index.

Dynamic elastic properties were tested according to the method of Liu et al. (2021). The gap was set to 1.0 nm, and the measurement was taken at 25 °C. For all samples, 1 % strain was completely within the linear viscoelastic range, so 1 % strain was selected to perform all dynamic measurements. The storage modulus (G') and loss modulus (G") were measured under 1 % oscillating strain from 0.1 rad/s to 100 rad/s.

2.9. Thermal property determination

Five milligrams of the mixture (dry basis) were weighed into an aluminum pan of a differential scanning calorimeter (DSC, Q2000, TA Instruments, USA), and 10 μL of deionized water was added. The lid was sealed, and the mixture was left at room temperature for 12 h. The temperature was increased from 30 °C to 120 °C at a rate of 10 °C /min, and the thermal properties were determined. The DSC program yields T_o (onset temperature), T_p (peak temperature), T_c (conclusion temperature), and ΔHg (gelatinization enthalpy). The ratio of gelatinization enthalpy (ΔHg) and retrogradation enthalpy (ΔHr) (ΔHr/ΔHg) is used to describe the retrogradation rate (R%).

2.10. Short-range ordered structure determination

The short-range ordered structure of all samples was measured using a Fourier transform infrared Spectrometer (VERTEX 70, Bruker, Germany) according to the experimental protocol of Zhou et al. (2019). The freeze-dried samples were ground and mixed with dry KBr. The mixed powder was ground again and pressed at a pressure of 15 MPa for about 1 min. The spectral range was 4000–400 cm^{-1}, the resolution was 4 cm^{-1}, and the number of scans was 64. The spectra were analyzed using the OMINIC software.

2.11. Gel hardness determination

Textural properties were determined according to the method of Zhong et al. (2020). Samples obtained by RVA were stored at 4 °C for 24 h, and gel hardness was measured using a texture analyzer (TA-XT, Stable Micro System, UK). A cylindrical probe (P 0.5) was used to measure all samples. The gel samples were cylindrical gels with a diameter of 36 mm and a height of 40 mm. The gels were compressed at a test speed of 1 mm/s with a trigger force of 5 g and a test distance of 10 mm.

2.12. X-ray diffraction

An X-ray diffractometer (D8 Advance, Bruker, Germany) was used to determine the gel samples after freeze-drying for 0 and 14 days stored at 4 °C. The measurement conditions were as follows: voltage 40 kV, current 40 mA. The scanning angle range was 5° to 40° (2θ), and the scanning speed was 3°/min. The diffraction pattern of the sample was analyzed using Jade 6.0 software.

2.13. In vitro starch digestibility

In vitro digestion of starch was assessed by the method of Englyst et al. (1992) with slight modifications. Firstly, a 500 mg sample was accurately weighed and mixed with 10 mL of acetate buffer (0.1 M, pH 5.2) and 6 glass beads to simulate gastrointestinal movement. The mixture was shaken up and bathed in water at 37 °C for 10 min. Add 2.5 mL of enzymatic solution and digest with shaking at 37 °C. Take 0.5 mL of the reaction solution at 0, 20, 40, 60, 90, and 120 min and add 20 mL of 66 % ethanol to stop the enzyme. After centrifugation, 0.1 mL of the supernatant was added to 3 mL of GOPOD (glucose kit solution) and reacted at 45 °C for 20 min. The rapid digestible starch (RDS), slowly digestible starch (SDS), and resistant starch (RS) were calculated based on the glucose measurement value and the hydrolysis rate, respectively, using the following formulas:

$$RDS(\%) = (G_{20} - G_0)/TS \times 0.9 \times 100 \quad (2)$$

$$SDS(\%) = (G_{120} - G_{20})/TS \times 0.9 \times 100 \quad (3)$$

$$RS(\%) = 100 - RDS(\%) - SDS(\%) \quad (4)$$

G_0, G_{20}, and G_{120} (mg) in the formula represent the glucose content released after 0 min, 20 min, and 120 min, respectively, and TS (mg) represents the total starch content.

2.14. Statistical data analysis

All experiments were repeated three times, and the results are expressed as the mean ± standard deviation. Analysis was performed using SPSS 25.0. All images and graphs were created using Origin 2018 software. Analysis of variance with Tukey's post hoc test was used to compare differences between samples. $p < 0.05$ was considered

Table 1
Monosaccharide composition and average molecular weight of SDFs.

Samples	Average M_w (Da)	Mannose (%)	Rhamnose (%)	Galacturonic acid (%)	Glucose (%)	Xylose (%)	Arabinose (%)
HM-SDF	36,824	4.20	2.69	28.49	4.10	28.60	31.91
LM-SDF	20,616	4.93	NM	4.92	2.51	40.50	47.15

Table 2
Effects of SDFs of different molecular weights on pasting properties and the rheological parameters of CS.

Samples	up			down			Hysteretic loop ($Pa.s^{-1}$)	Peak Viscosity (cP)	Trough Viscosity (cP)	Break down Viscosity (cP)	Final Viscosity (cP)	Setback Viscosity(cP)	Peak Time (min)	Pasting Temp (°C)	Leached amylose (mg/g)
	K ($Pa.s^n$)	n	R^2	K($Pa.s^n$)	n	R^2									
CS	168.44 ± 13.68^a	0.27 ± 0.02^b	0.984	68.30 ± 3.06^a	0.43 ± 0.01^a	0.990	19,066	2706 ± 61.65^a	1646.67 ± 43.25^a	1059.33 ± 31.07^a	2621.33 ± 57.35^a	974.67 ± 29.67^a	5.27 ± 0^b	79.15 ± 0^b	19.23 ± 0.35^a
CS-HM-SDF	105.41 ± 10.67^c	0.31 ± 0.02^a	0.985	48.22 ± 2.97^c	0.43 ± 0.01^a	0.989	8436	2525.67 ± 23.67^c	1689 ± 18.52^a	836.67 ± 18.15^c	2499.33 ± 30.37^b	810.33 ± 17.90^c	5.27 ± 0^b	79.95 ± 0^a	16.76 ± 0.32^c
CS-LM-SDF	141.26 ± 8.29^b	0.26 ± 0.01^b	0.983	56.99 ± 3.02^b	0.42 ± 0.01^a	0.989	15,911	2660.67 ± 23.67^b	1704.67 ± 45.09^a	956 ± 49.57^b	2586.33 ± 26.50^a	881.67 ± 27.43^b	5.27 ± 0^b	79.15 ± 0^b	18.39 ± 0.16^b

Note: Different letters in the table indicate significant differences ($p < 0.05$).

statistically significant.

3. Results and analysis

3.1. Composition and relative molecular mass of SDFs in different fractions

Gradient ethanol precipitation is an effective method for isolating SDFs with different molecular weight fractions (Fan et al., 2021). The monosaccharide composition and molecular weight of the SDF components obtained through this method are presented in Table 1. The modified high molecular weight soluble dietary fiber (HM-SDF), precipitated with 40 % ethanol, had an average molecular weight of 36,824 Da, significantly higher than that of the low molecular weight soluble dietary fiber (LM-SDF), which was 20,616 Da, obtained using 80 % ethanol. This difference demonstrates that ethanol disrupts the hydrogen bonds in the SDFs, causing components of varying molecular weights to precipitate. Additionally, the ethanol concentration is correlated with the molecular weight of the SDFs, and as the ethanol concentration increased, HM-SDF was precipitated first, followed by LM-SDF.

The monosaccharide composition of HM-SDF and LM-SDF, obtained at two different ethanol concentrations, varies significantly, as shown in Table 1. HM-SDF contains a notably higher amount of galacturonic acid (28.49 %) compared to LM-SDF (4.92 %), which aligns with the findings of Xue et al. (2019b) on graded ethanol precipitation. Xylose and arabinose, the primary components of hemicellulose, are present in both fibers. HM-SDF contains 28.6 % xylose and 31.91 % arabinose, while LM-SDF has 40.5 % xylose and 47.15 % arabinose. Ethanol is usually soluble in biomolecules such as polysaccharides and proteins. When ethanol is added gradually, the polarity of the solution changes, making these biomolecules less soluble. As the concentration of ethanol increases and reaches a certain level, these biomolecules precipitate out of the solution and form a precipitate. The polarity varies with the concentration of ethanol. This may explain the difference in monosaccharide composition(Cao et al., 2023). These results suggest that arabinoxylan is the main component of both HM-SDF and LM-SDF.

3.2. Effect of SDFs with different molecular weights on the pasting properties of CS

The pasting properties of starch are critical to its functionality, as they determine its ability to transform into a usable form, such as a paste or gel, which influences its application in food products. Table 2 shows the effect of adding 5 % SDFs (*W*/W, based on the dry weight of CS) with different molecular weights (HM-SDF and LM-SDF) on the pasting properties of corn starch (CS). The addition of SDFs reduced both the peak viscosity (PV) and final viscosity (FV) of CS, while the trough viscosity (TV) remained unchanged. This finding aligns with previous studies (Li, Liu, et al., 2022). During starch pasting, viscosity changes are influenced by starch-lipid complex formation, amylose leaching, interactions with other ingredients, and starch chain mobility in water. PV reflects the maximum viscosity of starch granules as they expand during heating, indicating amylopectin behavior. HM-SDF had a more significant inhibitory effect on CS pasting compared to LM-SDF. The PV of CS-HM-SDF decreased from 2706 cP to 2525.67 cP, while the PV of CS-LM-SDF only decreased to 2660.67 cP. This result is consistent with earlier studies on pectin-starch mixtures(Zhang et al., 2018). The hydrocolloid absorbs moisture, swells, and competes with starch granules for moisture, inhibiting starch swelling and reducing pasting viscosity. Similar trends were observed in a konjac glucomannan-CS system with varying molecular weights, where higher molecular weight SDFs had a stronger inhibitory effect on amylose leaching and starch granule swelling (*S. ma*, P. Zhu, M. Wang, et al., 2019). The FV value reflects the ability of starch to form a viscous mass. Similar to PV, the decrease in FV (122 cP) with HM-SDF addition was greater than the decrease caused by LM-SDF (35

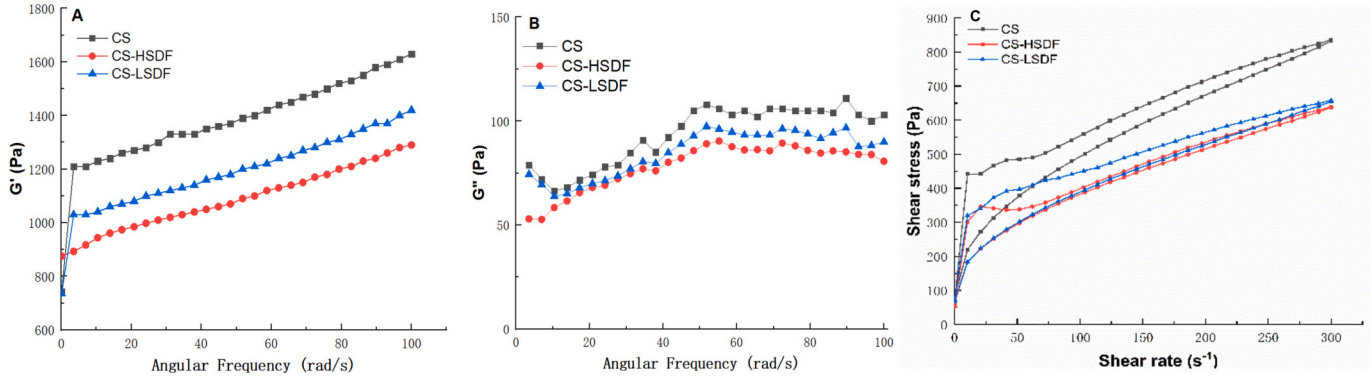

Fig. 1. Effects of different molecular weight SDFs on the dynamic rheological properties, Storage modulus G' (A) and loss modulus G" (B) and the static rheological properties (C) of CS.

cP), indicating that HM-SDF reduces the thickening ability of CS more effectively. HM-SDF disrupts the hydration film around starch particles, affecting moisture movement and inhibiting starch solubilization, which in turn reduces viscosity.

Adding LM-SDF did not significantly affect the starch pasting temperature, while HM-SDF notably increased the pasting temperature. This suggests that HM-SDF delays starch pasting more than LM-SDF. HM-SDF, with its higher viscosity and moisture absorption properties, forms a protective layer around the starch granules, preventing their disintegration during pasting and raising the pasting temperature.

The breakdown (BD) viscosity reflects starch integrity; a higher BD viscosity indicates weaker granule integrity. The reduction in BD viscosity was more pronounced with HM-SDF than LM-SDF, likely due to the higher molecular weight of HM-SDF, which inhibits amylose leaching more effectively and preserves starch granule integrity during shearing. The starch setback (SB) viscosity represents short-term retrogradation and is the difference between FV and TV. It indicates starch retrogradation during cooling and correlates with amylose leaching (Zhou et al., 2017). A lower SB viscosity suggests a lower rate of starch retrogradation. HM-SDF reduced the SB viscosity of CS from 974.67 cP to 810.33 cP, while LM-SDF only reduced it to 881.67 cP. This indicates that HM-SDF is more effective at reducing leaching of amylose and inhibiting short-term retrogradation(Cui et al., 2024).

3.3. Effect of SDFs with different molecular weights on the rheological properties of CS

3.3.1. Static rheological properties

The rheological properties of corn starch (CS) with 5 % HM-SDF and 5 % LM-SDF (*W*/W, based on the dry weight of CS) are shown in Fig. 1. Compared to NCS, both HM-SDF and LM-SDF reduced the viscosity of the starch paste. The rheological curves were fitted using the power law model (Table 2), with R^2 values exceeding 0.983, indicating a good fit. The n value for all samples was less than 1, confirming that all samples are non-Newtonian fluids exhibiting shear thinning and pseudoplasticity. The consistency coefficient (K) is a measure of starch viscosity. The K value was lowest for the HM-SDF sample, followed by LM-SDF, suggesting that HM-SDF is more effective than LM-SDF at reducing pasting viscosity and inhibiting short-term retrogradation. The decrease in K value is attributed to reduced intermolecular flow resistance, resulting from a lower proportion of long amylose (Lei et al., 2020). The SDFs interact with amylose, limiting its leaching and delaying the formation of hydrogen bonds, which results in lower viscosity, with HM-SDF being more effective in this regard. This trend was further confirmed in the RVA study. The thixotropic loop area, calculated by subtracting the area of the ascending curve from the descending curve, is inversely related to starch shear resistance (Wang et al., 2022). A smaller thixotropic loop area indicates stronger shear stability. The addition of HM-SDF and LM-SDF reduced the thixotropic loop area by 55.8 % and 16.5 %, respectively, indicating that HM-SDF is more effective in improving starch shear stability. The BD viscosity trend in the RVA test further supported this observation. The lower the amylose content, the lower the retrogradation rate, confirming the relationship between amylose content and starch retrogradation. Amylose content exhibited a significant reduction upon SDFs incorporation, with the most pronounced decrease observed following HM-SDF addition. This result showed that adding SDFs can inhibit the retrogradation of CS, and HM-SDF has optimal inhibitory effects.

3.3.2. Dynamic rheological properties

The dynamic gel rheology of the CS, CS-HM-SDF, and CS-LM-SDF systems is shown in Fig. 1(A-B). The storage modulus (G') and loss modulus (G") represent the elastic and viscous properties of the system, respectively (Gan et al., 2023). In starch-hydrocolloid mixtures, there is a strong correlation between angular frequency and elasticity, with higher angular frequencies leading to higher elasticity (G' > G") (Shahzad et al., 2019).

For all three samples, G' was significantly higher than G", indicating gel-like behavior and suggesting that all samples formed typical gels (Gan et al., 2023). Both G' and G" increased with frequency, displaying a dependency that is characteristic of weak gels (Wu et al., 2020). Adding HM-SDF and LM-SDF reduced the elasticity of gel, which is likely due to the inhibition of starch retrogradation by these fibers. Among the samples, the CS-HM-SDF gel exhibited the lowest elasticity. This is because short-term retrogradation primarily involves the rearrangement of amylose. The higher molecular weight of HM-SDF allows it to interact

Table 3
Effects of different molecular weight SDFs on the thermal properties of CS.

Samples	Gelatinization				Retrogradation				R(%)
	T_o (°C)	T_p (°C)	T_c (°C)	ΔHg (J/g)	T_{or} (°C)	T_{pr} (°C)	T_{cr} (°C)	ΔHr (J/g)	
CS	66.54 ± 0.05^b	70.44 ± 0.20^b	84.94 ± 0.07^a	12.24 ± 0.16^a	41.38 ± 0.57^b	56.02 ± 0.31^c	81.33 ± 0.75^a	7.95 ± 0.16^a	64.95
CS-HM-SDF	68.20 ± 0.21^a	72.10 ± 0.12^a	85.19 ± 0.06^a	10.93 ± 0.14^b	42.76 ± 0.24^a	55.49 ± 0.18^b	79.90 ± 0.03^b	6.28 ± 0.46^b	57.46
CS-LM-SDF	68.21 ± 0.05^a	72.37 ± 0.11^a	85.41 ± 0.12^a	11.39 ± 0.24^b	43.05 ± 0.64^a	58.57 ± 1.10^a	80.01 ± 0.52^b	5.07 ± 0.15^c	44.51

Note: Different letters in the table indicate significant differences ($p < 0.05$).

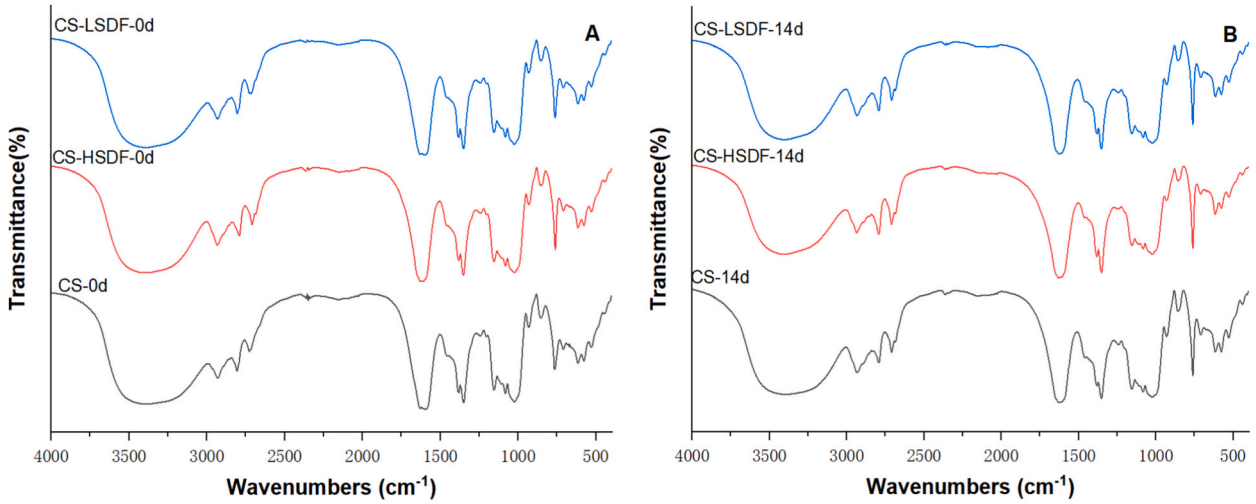

Fig. 2. Effects of different molecular weight SDFs on the FT-IR spectra of CS stored at 4 °C for 0 d (A) and 14 d (B).

more readily with amylose, reducing its leaching and inhibiting short-term retrogradation. This delays the formation of starch hydrogen bonds, resulting in the formation of a weaker gel. This finding is consistent with the SB viscosity observed in the RVA test.

3.4. Influence of SDFs with different molecular weights on the thermal properties of CS

The thermal properties of the pasting and retrogradation processes of CS with added HM-SDF and LM-SDF were analyzed using Differential Scanning Calorimetry (DSC), with results shown in Table 3. The addition of both HM-SDF and LM-SDF significantly increased the onset temperature of gelatinization (T_o) and peak temperature of gelatinization (T_p), indicating a delay in starch pasting (Yoo et al., 2015). This delay is attributed to the competition between the hydrophilic dietary fibers and starch molecules for moisture, which hinders moisture transfer to the starch and slows down the pasting process. The gelatinization enthalpy (ΔHg), which reflects the energy required for amylose gelatinization, decreased with the addition of HM-SDF and LM-SDF, from 12.24 J/g in the control to 10.93 J/g and 11.39 J/g, respectively. The CS-HM-SDF system showed the lowest ΔHg, suggesting that SDFs reduce the mobility and hydration of starch chains, thereby lowering the energy required for gelatinization (Yang et al., 2019). Additionally, the higher molecular weight of HM-SDF strengthens its interaction with amylose via hydrogen bonds, further inhibiting starch gelatinization, delaying the melting of the crystalline region, and reducing the ΔHg more effectively than LM-SDF (Yoo et al., 2015).

After 14 days of storage, the pasting temperature of all starch gels decreased. The retrogradation enthalpy (ΔHr) of the HM-SDF and LM-SDF systems dropped to 6.28 J/g and 5.07 J/g, respectively, indicating that reheating only partially melts the crystalline structure of the starch, resulting in lower enthalpy values. The degree of retrogradation (R-value), calculated as the ratio of ΔHr to ΔHg, reflects the extent of starch molecule ordering. CS exhibited a retrogradation rate of 64.95 %, while HM-SDF-CS and LM-SDF-CS showed reduced rates of 57.46 % and 44.51 %, respectively. This suggests that SDFs help reduce starch retrogradation, with LM-SDF being more effective than HM-SDF. These findings are consistent with previous studies, such as those by Wu et al. (2020), which compared the effects of extruded and untreated SDFs on rice starch retrogradation. Their results indicated that extruded SDFs, with higher LM-SDF content, were better at inhibiting long-term retrogradation, while untreated SDFs more effectively prevented short-term retrogradation.

Table 4
Effects of SDFs of different molecular weights on the short-range ordered structure and digestibility of CS stored at 4 °C for 0 d and 14 d.

Samples	Storage time	R1047/1022	R995/1022	RDS (%)	SDS(%)	RS(%)
CS	0 d	0.6879 ± 0.001	0.7114 ± 0.002	70.90 ± 0.19^{a}	16.27 ± 0.23^{d}	12.83 ± 0.11^{e}
	14 d	0.7688 ± 0.006	0.8536 ± 0.007	68.19 ± 0.58^{c}	17.18 ± 0.15^{bc}	14.63 ± 0.54^{c}
CS-HM-SDF	0 d	0.6502 ± 0.003	0.6937 ± 0.002	68.26 ± 0.31^{c}	17.47 ± 0.42^{ab}	14.27 ± 0.24^{c}
	14 d	0.7202 ± 0.002	0.7984 ± 0.002	64.84 ± 0.15^{e}	17.75 ± 0.21^{a}	17.41 ± 0.33^{a}
CS-LM-SDF	0 d	0.6746 ± 0.001	0.7029 ± 0.015	69.60 ± 0.21^{b}	16.84 ± 0.08^{c}	13.55 ± 0.28^{d}
	14 d	0.6972 ± 0.001	0.7921 ± 0.003	66.58 ± 0.41^{d}	17.34 ± 0.31^{abc}	16.08 ± 0.10^{b}

Note: Different letters in the table indicate significant differences ($p < 0.05$).

3.5. Effect of SDFs with different molecular weights on CS Fourier transform infrared spectroscopy

The FTIR spectra of various samples are presented in Fig. 2 No new peaks appeared in the FTIR spectra of CS with the addition of HM-SDF and LM-SDF at both 0 and 14 days, indicating that no new covalent bonds were formed between the SDFs and CS. However, the spectra showed a shift to a lower wave number, suggesting that the primary interaction between SDFs and CS is through hydrogen bonding (He et al., 2020). The FTIR spectra were deconvoluted using OMNIC software, and the resulting data are summarized in Table 4. The absorbance ratio of 1047 cm^{-1} to 1022 cm^{-1} (1047/1022) is used to assess the short-range ordered structure of starch molecules. A higher ratio indicates more excellent crystallinity and order. The addition of both HM-SDF and LM-SDF reduced the 1047/1022 ratio from 0.6879 in the control to 0.6502 and 0.6746, respectively, suggesting that HM-SDF is more effective than LM-SDF in reducing the short-range ordered structure of starch. These findings align with the results from the RVA and dynamic rheology tests. The observed decrease in the ratio may be attributed to two factors. SDFs bind to leached amylose through hydrogen bonds and moisture loss, which inhibits amylopectin retrogradation (Tang et al., 2013).

The absorbance ratio at 995 cm^{-1} and 1022 cm^{-1} (995/1022) reflects the order of the double-helix structure within the starch crystalline regions. A higher ratio indicates a more ordered double-helix structure. After 14 days of storage, both the 1047/1022 and 995/1022 ratios

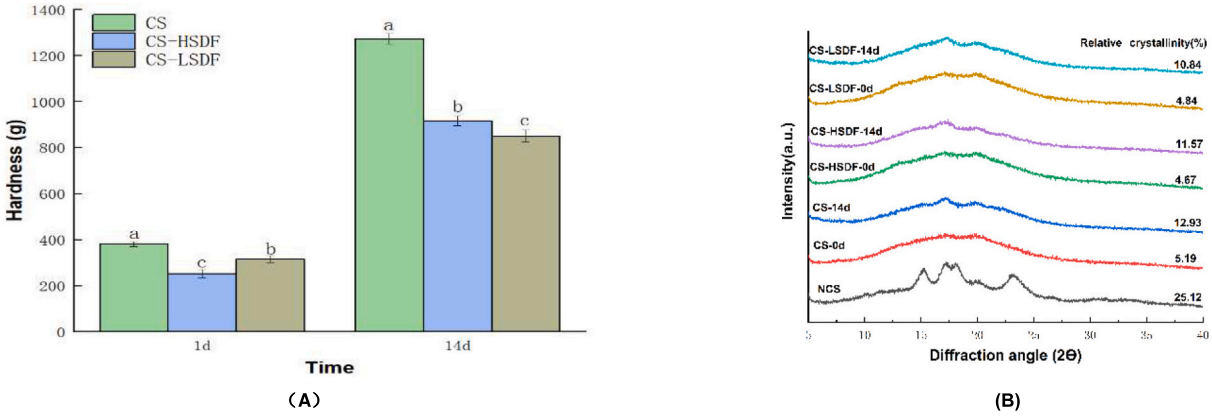

Fig. 3. Effects of different molecular weight SDFs on gels hardness of CS stored at 4 °C for 1 d and 14 d (A) and the crystallinity of CS stored at 4 °C for 0 d and 14 d (B).

increased from 0.6879 and 0.7114 to 0.7688 and 0.8536, respectively, indicating an increase in starch order due to the recrystallization of amylopectin during retrogradation. SDFs indirectly inhibit amylopectin recrystallization by weakening amylose pasting. The values for LM-SDF at both 1047/1022 and 995/1022 after 14 days were significantly lower than those for HM-SDF, suggesting that LM-SDF is more effective in inhibiting the long-term retrogradation of starch. LM-SDF is more likely to integrate into the starch structure during retrogradation, increasing the distance between starch molecules and delaying the formation of hydrogen bonds (D. Luo et al., 2017).

3.6. Effect of SDFs with different molecular weights on the texture properties of CS

Gel hardness is a critical parameter for gel-based foods, with amylose rearrangement, rather than amylopectin degradation, being the main factor in starch gel formation. Starch retrogradation increases the hardness of starch gels. The changes in the gel hardness of CS with the addition of HM-SDF and LM-SDF are shown in Fig. 3 (A). Adhesion between starch molecules, along with gel hardness and compactness, are positively correlated with starch retrogradation. Both HM-SDF and LM-SDF significantly reduced the hardness of CS gels. After 1 day of storage, the gel hardness decreased from 380.69 g to 251.95 g for HM-SDF and 314.98 g for LM-SDF. This reduction is attributed to the inhibition of starch recrystallization by SDFs. The gel hardness of HM-SDF-CS was lower than that of LM-SDF-CS, as HM-SDF more effectively inhibits amylose leaching, resulting in stronger short-term retrogradation inhibition. Consequently, HM-SDF reduces the degree of starch ordering, making the network structure of the gel less rigid compared to the CS and CS-LM-SDF gels. After 14 days of storage, the gel hardness of CS increased significantly, from 380.69 g to 1272.9 g, due to long-term retrogradation involving amylopectin recrystallization and the formation of hydrogen bonds. In contrast, the gel hardness of CS-HM-SDF and CS-LM-SDF was reduced to 917.05 g and 851.12 g, respectively, indicating that both HM-SDF and LM-SDF effectively reduce gel hardness during prolonged storage. Notably, LM-SDF was more effective than HM-SDF in reducing gel hardness, suggesting that LM-SDF better inhibits long-term starch retrogradation and the recrystallization of amylopectin, thereby limiting hydrogen bond formation between starch chains. Previous studies have linked changes in gel hardness and dehydration shrinkage in starch-dietary fiber mixtures to the plasticizing effect of dietary fiber. Both dietary fiber and moisture have a plasticizing effect on starch, but when dietary fiber exerts a stronger plasticizing effect than moisture, it promotes starch recrystallization. Conversely, when the plasticizing effect of dietary fiber is weaker, it inhibits the ordered arrangement of starch molecules. Additionally, starch retrogradation often results in dehydration, increased crystallinity, and thicker gel cell walls, all contributing to increased gel hardness. LM-SDF, due to its greater inhibitory effect on retrogradation, is more effective at reducing gel hardness by slowing these processes (Zhou et al., 2021).

3.7. Effect of SDFs with different molecular weights on the crystal structure of CS

The X-ray diffraction patterns and crystallinity of HM-SDF and LM-SDF, both stored for 0 and 14 days, are shown in Fig. 3 (B). NCS exhibits diffraction peaks at 15°, 17°, 18°, and 23°, characteristic of a typical A-type crystal structure. However, pasting disrupts the crystalline region of starch, leading to a decrease in crystallinity. All gels showed diffraction peaks at 17° and 20°, indicating a shift to a B-type crystal structure after pasting. During short-term retrogradation (0 days), HM-SDF reduced the relative crystallinity (RC) from 5.19 % to 4.67 %, which was significantly lower than LM-SDF's RC of 4.84 %. This suggests that HM-SDF is more effective in inhibiting short-term retrogradation.

After 14 days of storage (long-term retrogradation), the RC of LM-SDF (6 %) remained lower than that of HM-SDF (6.9 %), indicating that LM-SDF is more effective in preventing long-term retrogradation. The reduction in RC is likely due to the formation of hydrogen bonds between SDFs and starch molecules, which inhibits the formation of ordered structures during retrogradation (Zhang et al., 2018). Similar findings were observed in studies investigating the impact of non-starch polysaccharides of varying molecular weights on yam starch (Huang et al., 2023). These results suggest that HM-SDF is more effective at inhibiting amylose recrystallization, while LM-SDF better inhibits amylopectin recrystallization. This aligns with the findings from RVA and FTIR spectroscopy analyses.

3.8. Effect of SDFs with different molecular weights on the in vitro digestion properties of CS

The digestion properties of starch mixtures with added HM-SDF and LM-SDF, stored for different durations, are summarized in Table 4. After 0 days of storage, the addition of HM-SDF and LM-SDF significantly reduced the RDS content from 70.90 % to 68.26 % and 69.60 %, respectively, while increasing the proportion of SDS and RS. This indicates that SDFs effectively slow starch digestion. Notably, HM-SDF had a more pronounced effect than LM-SDF, likely due to its higher molecular weight. When hydrated, HM-SDF forms a stronger encapsulating effect around starch and enzymes, whereas LM-SDF, being more water-soluble and dispersible, does not exhibit the same level of encapsulation. After 14 days of storage, starch retrogradation further

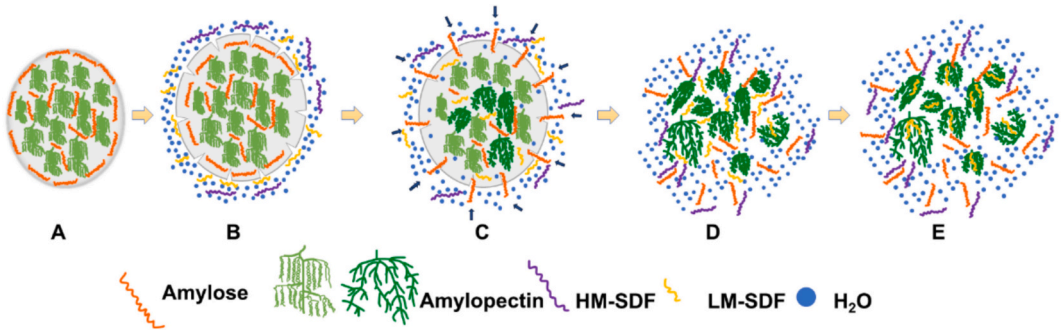

Fig. 4. Model of the mechanism of SDFs participating in starch pasting and retrogradation. Natural starch granules. (A) Starch granules undergo moisture-absorption swelling under heating conditions. (B) SDFs were wrapped around the surface of the starch granules. When swelling reached a certain level, the starch granules disintegrated, amylose was released, the ordered structure of amylopectin was destroyed, HM-SDF interacted with amylose by hydrogen bonding, and LM-SDF entered the starch granules. (C) The starch granules completely disintegrated. (D) LM-SDF was inserted into the amylopectin molecular chain and inhibited the formation of the long-range ordered structure of the starch. (E).

decreased RDS and increased SDS and RS. This was attributed to the reorganization of amylopectin into a more ordered structure, leading to larger crystalline regions. These structural changes, occurring during long-term storage at 4 °C, contributed to a reduction in the digestibility of CS.

4. Mechanism analysis of the inhibition of starch retrogradation by SDFs with different molecular weights

The mechanism by which SDFs influence starch properties (Fig. 4) differs from traditional enzymatic or chemical modifications. Instead of altering the molecular structure of starch, SDFs affect its processing properties through competitive moisture absorption, physical encapsulation, and hydrogen bonding interactions. When comparing HM-SDF and LM-SDF, the addition of HM-SDF more effectively limits the leaching of amylose during starch pasting, resulting in a greater reduction in starch viscosity. FT-IR, DSC, XRD, and texture analyses confirm that HM-SDF is more effective at reducing the formation of short-range ordered structures in starch molecules. In contrast, LM-SDF is more effective in inhibiting long-term starch retrogradation. Based on the findings of this study, we propose a mechanism by which SDFs of different molecular weights interact with starch. In the presence of SDFs, starch granules begin to expand and rupture as the temperature increases, releasing amylose. HM-SDF acts by encapsulating the starch granules, limiting moisture availability and thus reducing amylose leaching. LM-SDF, on the other hand, inserts itself into the starch granules, forming hydrogen bonds with amylopectin and preventing the entanglement of starch molecules. Consequently, SDFs with varying molecular weight distributions exert different effects on starch retrogradation.

5. Conclusion

This study examines the effects and mechanisms of soluble dietary fibers with different molecular weights on the processing, retrogradation, and digestion properties of CS. HM-SDF more effectively inhibits the leaching and pasting of amylose in CS, whereas LM-SDF is superior in preventing long-term retrogradation. Overall, HM-SDF more efficiently restricts the processing, retrogradation, and digestion of CS. The interaction mechanisms between SDFs and starch are distinct for HM-SDF and LM-SDF. HM-SDF encapsulates the starch granules, limiting moisture absorption, swelling, pasting, and digestion. In contrast, LM-SDF penetrates the starch structure, hindering the formation of long-range ordered structures and delaying long-term retrogradation. This research provides a strategy for regulating starch behavior—specifically pasting, retrogradation, and digestion—through the use of SDFs with varying molecular weights. Additionally, it offers new insights into the application of dietary fiber in starch-based food products, highlighting the potential for tailored modifications to enhance food quality and stability.

CRediT authorship contribution statement

Yuqian Zheng: Writing – original draft, Software, Data curation. **Lixin You:** Software. **Wenyan Wang:** Software. **Xiaoyan Qin:** Software. **Zhilong Chen:** Software. **Ruining Zhang:** Software. **Jun Zhao:** Supervision, Funding acquisition, Conceptualization. **Sheng Li:** Writing – original draft, Supervision, Funding acquisition, Conceptualization.

Declaration of competing interest

The authors declare that they have no known competing financial interests or personal relationships that could have appeared to influence the work reported in this paper.

Acknowledgment

This work was supported by grants from the “Climbing plan projects of Changchun University” (ZKP202301), the “Science and Technology Research Program of Education Department of Jilin Province of China” (JJKH20240750KJ), and the “Key R&D Program of Jilin Provincial Department of Science and Technology” (20240303046NC).

Data availability

Data will be made available on request.

References

Bhatta, A. (2023). *Effects of soluble and insoluble fibres on pasting and retrogradation of wheat flour and quality of bread*.

Cao, F., Zhang, H., Yan, Y., Chang, Y., & Ma, J. (2023). Extraction of polysaccharides from Maca enhances the treatment effect of 5-FU by regulating CD4+T cells. *Heliyon, 9*(6), Article e16495. https://doi.org/10.1016/j.heliyon.2023.e16495

Cui, Y., Li, X., Sun, D., Guo, L., Cui, B., Zou, F., & Sun, C. (2024). Retrogradation inhibition of starches in staple foods with maltotetraose-forming amylase. *Food Chemistry, 15*, 449. https://doi.org/10.1016/j.foodchem.2024.139232

Englyst, H. N., Kingman, S. M., & Cummings, J. H. (1992). Classification and measurement of nutritionally important starch fractions. *European Journal of Clinical Nutrition, 46 Suppl 2*, S33–S50. ://MEDLINE:1330528.

Fan, R., Mao, G., Xia, H., & Zeng, J. (2021). Chemical elucidation and rheological properties of a pectic polysaccharide extracted from Citrus medica L. fruit residues by gradient ethanol precipitation. *International Journal of Biological Macromolecules, 198*, 46–53. https://doi.org/10.1016/j.ijbiomac.2021.12.131

Fatimah, S., Hafied, M. A., Indiasih, P. A. Y., Airlangga, B., Minah, F. N., Hudha, M. I., & Sumarno, S. (2024). Production of resistant starch type 3 from cassava starch with high shear mixing and centrifugation treatment to increase its total dietary fibre content. *International Journal of Food Science & Technology, 59*(10), 7818–7826. https://doi.org/10.1111/ijfs.17011

Funami, T., Kataoka, Y., Omoto, T., Goto, Y., Asai, I., & Nishinari, K. (2005). Effects of non-ionic polysaccharides on the gelatinization and retrogradation behavior of wheat starch. *Food Hydrocolloids, 19*(1), 1–13. https://doi.org/10.1016/j.foodhyd.2004.04.024

Gan, J., Huang, Z., Yu, Q., Peng, G., Chen, Y., Xie, J., & Xie, M. (2020). Microwave assisted extraction with three modifications on structural and functional properties of soluble dietary fibers from grapefruit peel. *Food Hydrocolloids, 101*, Article 105549. https://doi.org/10.1016/j.foodhyd.2019.105549

Gan, Z., Zhang, M., Xu, S., Li, T., Zhang, X., Wang, J., & Wang, L. (2023). Comparison of quinoa and highland barley derived dietary fibers influence on the physicochemical properties and digestion of rice starch. *Food Research International, 174*. https://doi.org/10.1016/j.foodres.2023.113549

He, H., Chi, C., Xie, F., Li, X., Liang, Y., & Chen, L. (2020). Improving the in vitro digestibility of rice starch by thermomechanically assisted complexation with guar gum. *Food Hydrocolloids, 102*. https://doi.org/10.1016/j.foodhyd.2019.105637

Huang, J., Yu, M., Wang, S., & Shi, X. (2023). Effects of jicama (Pachyrhizus erosus L.) non-starch polysaccharides with different molecular weights on structural and physicochemical properties of jicama starch. *Food Hydrocolloids, 139*, Article 108502. https://doi.org/10.1016/j.foodhyd.2023.108502

Jia, Z., Luo, Y., Barba, F. J., Wu, Y., Ding, W., Xiao, S., & Fu, Y. (2022). Effect of β-cyclodextrins on the physical properties and anti-staling mechanisms of corn starch gels during storage. *Carbohydrate Polymers, 284*, Article 119187. https://doi.org/10.1016/j.carbpol.2022.119187

Lee, D.-J., Park, E. Y., & Lim, S.-T. (2019). Effects of partial debranching and storage temperature on recrystallization of waxy maize starch. *International Journal of Biological Macromolecules, 140*, 350–357. https://doi.org/10.1016/j.ijbiomac.2019.08.128

Lei, N., Chai, S., Xu, M., Ji, J., Mao, H., Yan, S., & Sun, B. (2020). Effect of dry heating treatment on multi-levels of structure and physicochemical properties of maize starch: A thermodynamic study. *International Journal of Biological Macromolecules, 147*, 109–116. https://doi.org/10.1016/j.ijbiomac.2020.01.060

Li, S., Hu, N., Zhu, J., Zheng, M., Liu, H., & Liu, J. (2022). Influence of modification methods on physicochemical and structural properties of soluble dietary fiber from corn bran. *Food Chemistry: X, 14*, Article 100298. https://doi.org/10.1016/j.fochx.2022.100298

Li, S., Liu, H., Zheng, Q., Hu, N., Zheng, M., & Liu, J. (2022). Effects of soluble and insoluble dietary Fiber from corn bran on pasting, thermal, and structural properties of corn starch. *Starch - Stärke, 74*(5–6), 2100254. https://doi.org/10.1002/star.202100254

Liu, C., Zhang, H., Chen, R., Chen, J., Liu, X., Luo, S., & Chen, T. (2021). Effects of creeping fig seed polysaccharide on pasting, rheological, textural properties and in vitro digestibility of potato starch. *Food Hydrocolloids, 118*. https://doi.org/10.1016/j.foodhyd.2021.106810

Liu, X., Liu, S., Xi, H., Xu, J., Deng, D., & Huang, G. (2019). Effects of soluble dietary fiber on the crystallinity, pasting, rheological, and morphological properties of corn resistant starch. *LWT, 111*, 632–639. https://doi.org/10.1016/j.lwt.2019.01.059

Luo, D., Li, Y., Xu, B., Ren, G., Li, P., Li, X., & Liu, J. (2017). Effects of inulin with different degree of polymerization on gelatinization and retrogradation of wheat starch. *Food Chemistry, 229*, 35–43. https://doi.org/10.1016/j.foodchem.2017.02.058

Luo, S., Chen, R., Huang, L., Liang, R., Liu, C., & Chen, J. (2017). Investigation on the influence of pectin structures on the pasting properties of rice starch by multiple regression. *Food Hydrocolloids, 63*, 580–584. https://doi.org/10.1016/j.foodhyd.2016.10.016

Ma, S., Zhu, P., & Wang, M. (2019). Effects of konjac glucomannan on pasting and rheological properties of corn starch. *Food Hydrocolloids, 89*, 234–240. https://doi.org/10.1016/j.foodhyd.2018.10.045

Ma, S., Zhu, P., Wang, M., Wang, F., & Wang, N. (2019). Effect of konjac glucomannan with different molecular weights on physicochemical properties of corn starch. *Food Hydrocolloids, 96*, 663–670. https://doi.org/10.1016/j.foodhyd.2019.06.014

Ma, Y.-S., Pan, Y., Xie, Q.-T., Li, X.-M., Zhang, B., & Chen, H.-Q. (2019). Evaluation studies on effects of pectin with different concentrations on the pasting, rheological and digestibility properties of corn starch. *Food Chemistry, 274*, 319–323. https://doi.org/10.1016/j.foodchem.2018.09.005

Shahzad, S. A., Hussain, S., Alamri, M. S., Mohamed, A. A., & Qasem, A. A. A. (2019). Use of hydrocolloid gums to modify the pasting, thermal, rheological, and textural properties of sweet potato starch. *International Journal of Polymer Science, 2019*(4), 1–11. https://doi.org/10.1155/2019/6308591

Tang, M., Hong, Y., Gu, Z., Zhang, Y., & Cai, X. (2013). The effect of xanthan on short and long-term retrogradation of rice starch. *Starch - Stärke, 65*(7–8). https://doi.org/10.1002/star.201200170

Wang, N., Wu, L., Zhang, F., Kan, J., & Zheng, J. (2022). Modifying the rheological properties, in vitro digestion, and structure of rice starch by extrusion assisted addition with bamboo shoot dietary fiber. *Food Chemistry, 375*. https://doi.org/10.1016/j.foodchem.2021.131900

Wu, B., Degner, B., & McClements, D. J. (2013). Microstructure & rheology of mixed colloidal dispersions: Influence of pH-induced droplet aggregation on starch granule-fat droplet mixtures. *Journal of Food Engineering, 116*(2), 462–471. https://doi.org/10.1016/j.jfoodeng.2012.12.020

Wu, N. N., Qiao, C. C., Tian, X. H., Tan, B., & Fang, Y. (2020). Retrogradation inhibition of rice starch with dietary fiber from extruded and unextruded rice bran. *Food Hydrocolloids, 113*(3), Article 106488. https://doi.org/10.1016/j.foodhyd.2020.106488

Xue, Z., Chen, Y., Jia, Y., Wang, Y., Lu, Y., Chen, H., & Zhang, M. (2019a). Structure, thermal and rheological properties of different soluble dietary fiber fractions from mushroom Lentinula edodes (Berk.) Pegler residues. *Food Hydrocolloids, 95*, 10–18. https://doi.org/10.1016/j.foodhyd.2019.04.015

Xue, Z., Chen, Y., Jia, Y., Wang, Y., Lu, Y., Chen, H., & Zhang, M. (2019b). Structure, thermal and rheological properties of different soluble dietary fiber fractions from mushroom Lentinula edodes (Berk.) Pegler residues. *Food Hydrocolloids, 95*(OCT.), 10–18. https://doi.org/10.1016/j.foodhyd.2019.04.015

Yang, C., Zhong, F., Douglas Goff, H., & Li, Y. (2019). Study on starch-protein interactions and their effects on physicochemical and digestible properties of the blends. *Food Chemistry, 280*, 51–58. https://doi.org/10.1016/j.foodchem.2018.12.028

Yoo, B., & Sun, & D.. (2015). Effect of tapioca starch addition on rheological, thermal, and gelling properties of rice starch. *Lwt Food Science & Technology, 64*(1), 205–211. https://doi.org/10.1016/j.lwt.2015.05.062

Zhang, B., Bai, B., Pan, Y., Li, X. M., Cheng, J. S., & Chen, H. Q. (2018). Effects of pectin with different molecular weight on gelatinization behavior, textural properties, retrogradation and in vitro digestibility of corn starch. *Food Chemistry, 264*(OCT.30), 58–63. https://doi.org/10.1016/j.foodchem.2018.05.011

Zhao, Q., Tian, H., Chen, L., Zeng, M., Qin, F., Wang, Z., & Chen, J. (2021). Interactions between soluble soybean polysaccharide and starch during the gelatinization and retrogradation: Effects of selected starch varieties. *Food Hydrocolloids, 118*. https://doi.org/10.1016/j.foodhyd.2021.106765

Zheng, M., You, Q., Lin, Y., Lan, F., Luo, M., Zeng, H., & Zhang, Y. (2019). Effect of guar gum on the physicochemical properties and in vitro digestibility of lotus seed starch. *Food Chemistry, 272*, 286–291. https://doi.org/10.1016/j.foodchem.2018.08.029

Zhong, Y., Xiang, X., Chen, T., Zou, P., Liu, Y., Ye, J., & Liu, C. (2020). Accelerated aging of rice by controlled microwave treatment. *Food Chemistry, 323*. https://doi.org/10.1016/j.foodchem.2020.126853

Zhou, D., Ma, Z., Yin, X., Hu, X., & Boye, J. I. (2019). Structural characteristics and physicochemical properties of field pea starch modified by physical, enzymatic, and acid treatments. *Food Hydrocolloids, 93*, 386–394. https://doi.org/10.1016/j.foodhyd.2019.02.048

Zhou, D. N., Zhang, B., Chen, B., & Chen, H. Q. (2017). Effects of oligosaccharides on pasting, thermal and rheological properties of sweet potato starch. *Food Chemistry, 230*(SEP.1), 516–523. https://doi.org/10.1016/j.foodchem.2017.03.088

Zhou, J., Jia, Z., Wang, M., Wang, Q., Barba, F. J., Wan, L., & Fu, Y. (2022). Effects of Laminaria japonica polysaccharides on gelatinization properties and long-term retrogradation of wheat starch. *Food Hydrocolloids, 133*. https://doi.org/10.1016/j.foodhyd.2022.107908

Zhou, R., Wang, Y., Wang, Z., Liu, K., Wang, Q., & Bao, H. (2021). Effects of Auricularia auricula-judae polysaccharide on pasting, gelatinization, rheology, structural properties and in vitro digestibility of kidney bean starch. *International Journal of Biological Macromolecules, 191*, 1105–1113. https://doi.org/10.1016/j.ijbiomac.2021.09.110